communications biology

A Nature Portfolio journal

Article

https://doi.org/10.1038/s42003-025-08211-8

Unraveling the roles of spatial working memory sustained and selective neurons in prefrontal cortex

Check for updates

Mohammad Aliramezani[1], Christos Constantinidis[2] & Mohammad Reza Daliri[1,3]

The heart of goal-directed behavior organization is working memory. Recent studies have emphasized the critical role of the prefrontal cortex (PFC) in working memory, highlighting elevated spiking levels in PFC neurons during working-memory delays. As a higher-order cortex, PFC contains various types of neurons with complex receptive fields, making it challenging to identify task-engaged neurons, particularly during the working memory periods when firing rates are lower compared to stimulus periods. While previous studies have primarily focused on neurons selective for sensory stimuli, there are also task-sustained neurons that are not selective for specific stimulus characteristics. In this study, we differentiate between working memory (WM)-sustained neurons, which show task-related activity without stimulus spatial selectivity, and working memory (WM)-selective neurons, which are selective for the location of the stimulus. To investigate their roles, we investigated the neural activities of the lateral PFC neurons in two macaque monkeys during a spatial working memory task. Fano factor analysis revealed that the neuronal variability of both WM-selective and WM-sustained neurons was similar and significantly higher than that of non-active neurons (neurons not modulated by the task). Moreover, the Fano factor of active neurons diminished during error trials compared to correct trials. The spike phase locking (SPL) value was measured to evaluate the coupling of local field potentials (LFPs) phases to spike times, considering neural network characteristics. SPL results indicated that both WM-selective neurons and WM-sustained neurons exhibited higher SPL in the alpha/beta-band compared to non-active neurons. Additionally, the alpha/beta-band SPL of working memory-active neurons decreased during error trials. In summary, despite the non-stimulus-specific activation of WM-sustained neurons, they may contribute to task performance alongside WM-selective neurons.

The ability to retain and manipulate information in mind for a short period over time is known as working memory, and it is essential to executive functions[1,2]. Working memory has been the subject of extensive research due to its crucial role in goal-directed behaviors and cognitive flexibility[3–7].

In nonhuman primates, neurophysiological studies revealed neurons that respond to sensory stimuli and keep firing even after a stimulus stops being present. This phenomenon, known as "persistent activity" or "delay activity" has been linked to the neurological basis of working memory[8–10]. In other words, the persistent activity that maintains neural populations active is reflected in delay activity. Though persistent activity can arise from single-neuron mechanisms, it has been suggested that neuron activation has been sustained by recurrent connections in a network of neurons[11,12].

A large portion of cortex is involved in working memory including posterior cortical regions that support maintaining particular content, as well as the frontal cortex which is associated with executive tasks[2,13]. Furthermore, earlier studies revealed that neurons in higher-order cortex, including the prefrontal cortex (PFC), show delay activity[8,9].

Persistent activity in the PFC has been demonstrated to encode information other than the physical properties of stimuli. For example, persistent activity can reflect stimulus category[14–16], numerical concepts[17], and abstract rules of the cognitive task[18,19]. Moreover, the persistent activity of single neurons has the potential to represent information related to the animal's prior experience. Hence, it has been suggested that persistent activity also plays an important role in learning procedure[20–23].

[1]School of Cognitive Sciences (SCS), Institute for Research in Fundamental Sciences (IPM), Tehran, Iran. [2]Department of Biomedical Engineering, Vanderbilt University, Nashville, TN, USA. [3]Department of Biomedical Engineering, School of Electrical Engineering, Iran University of Science and Technology (IUST), Tehran, Iran. e-mail: Daliri@iust.ac.ir

In persistent activity phenomena, some neurons either become active or stay activated after the stimulus offset. These neurons are believed to represent stimulus or task features to be used in further task procedures. We can categorize neurons with elevated activity in the absence of stimulus as WM-sustained neurons and WM-selective neurons. WM-sustained neurons refer to neurons that are activated in the working memory periods relative to before the stimulus onset (i.e., the fixation epoch). It is noteworthy that sustained neurons are not necessarily selective for a specific feature of the stimulus (for example, the location of the stimulus). In contrast, WM-selective neurons exhibit significantly increased activity in response to a feature of the presented stimulus in the working memory period (i.e., after the stimulus offset).

Most previous studies have considered WM-selective neurons to address the role of persistent activity in working memory, because they capture stimulus characteristics more accurately. Since WM-sustained neurons are not exclusively feature-selective, their roles are not well understood during working memory. In this study, we aimed to compare the roles of WM-sustained and WM-selective neurons in working memory task and uncover the probable functions of them.

Results

In the current study, two macaque monkeys were trained on a delayed match-to-sample task. There were nine possible locations for the white square on a 3×3 grid in the stimulus set. Each trial featured two spatial stimuli presented sequentially, with a 1500 ms delay between them. After the second delay, the fixation point disappeared, and two target alternatives appeared on the screen (Fig. 1). The monkeys had to saccade to the green or blue target, depending on whether the two stimuli matched or did not match. To obtain a reward of a drop of juice, the monkeys were required to attend, retain the location of the first stimulus in working memory, compare it with the location of the second stimulus, and correctly report the matching status of stimuli. Spiking activities and local field potentials (LFPs) were recorded from three PFC subdivisions: the posterior-dorsal, mid-dorsal, and posterior-ventral prefrontal cortex[23,24].

The first analysis was performed to identify WM-sustained neurons from 850 recorded neurons (171 in the posterior-dorsal, 321 in the mid-dorsal, and 358 in the posterior-ventral). Neurons with elevated spiking activity during the first and second delay periods, compared to the 1-s fixation period were identified as WM-sustained neurons (Wilcoxon signed-rank test, $p < 0.05$). A total of 233 neurons (38/171 [22.2%] in the posterior-dorsal, 96/321 [29.9%] in the mid-dorsal, and 99/358 [27.7%] in the posterior-ventral) and 191 neurons (45/171 [26.3%] in the posterior-dorsal, 80/321 [24.9%] in the mid-dorsal, and 66/358 [18.4%] in the posterior-ventral) were WM-sustained based on firing rate during the first and second delay periods, respectively. In contrast, 449 neurons (92/171 [53.8%] in the posterior-dorsal, 148/321 [46.1%] in the mid-dorsal, and 209/358 [58.4%] in the posterior-ventral) were classified as non-sustained, as they did not exhibit elevated firing activity in any task epoch.

Secondly, the firing rates during the working memory epochs (the first and the second delay periods, analyzed separately) were statistically

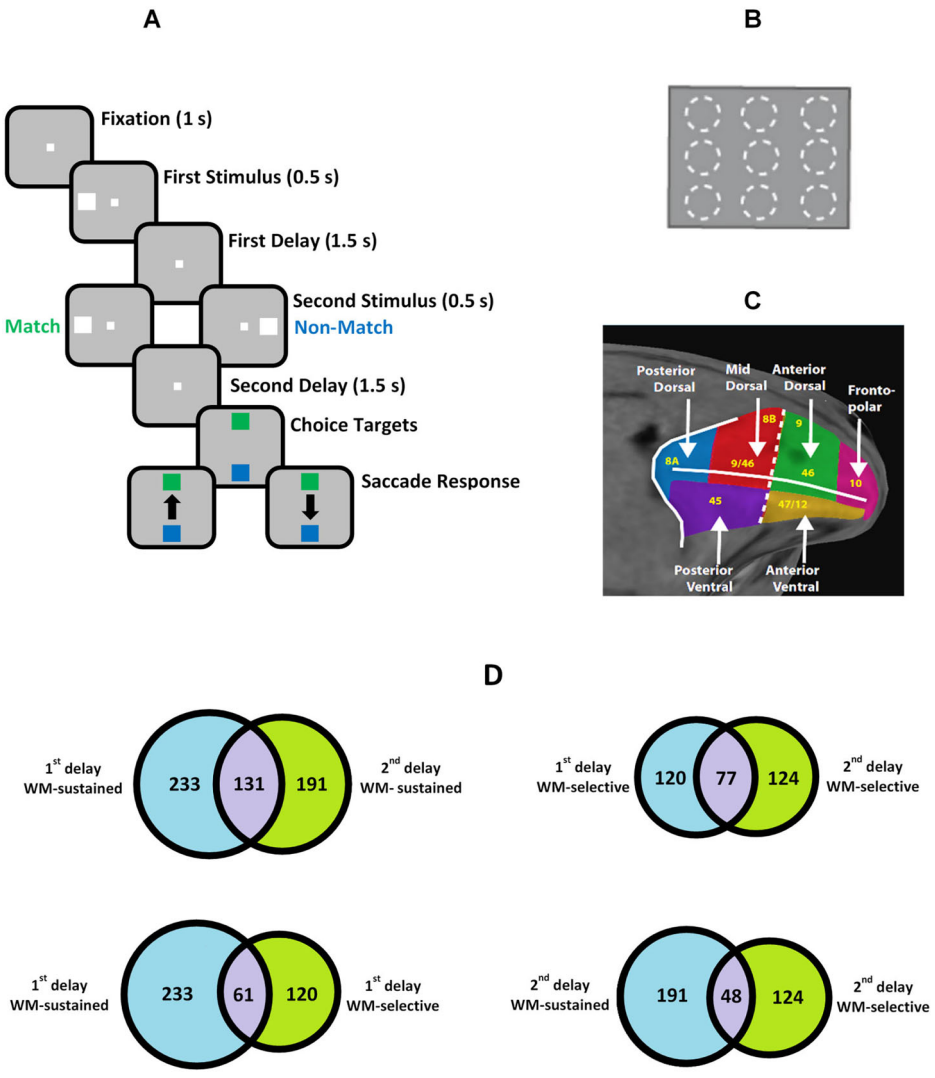

Fig. 1 | Behavioral spatial working memory task. **A** Task procedure: Monkeys were trained to determine if the first and second stimuli matched or did not match in terms of location. **B** Nine potential stimulus locations in the task. **C** The anatomical PFC subdivisions. **D** Number of WM-sustained and WM-selective neurons in each delay period.

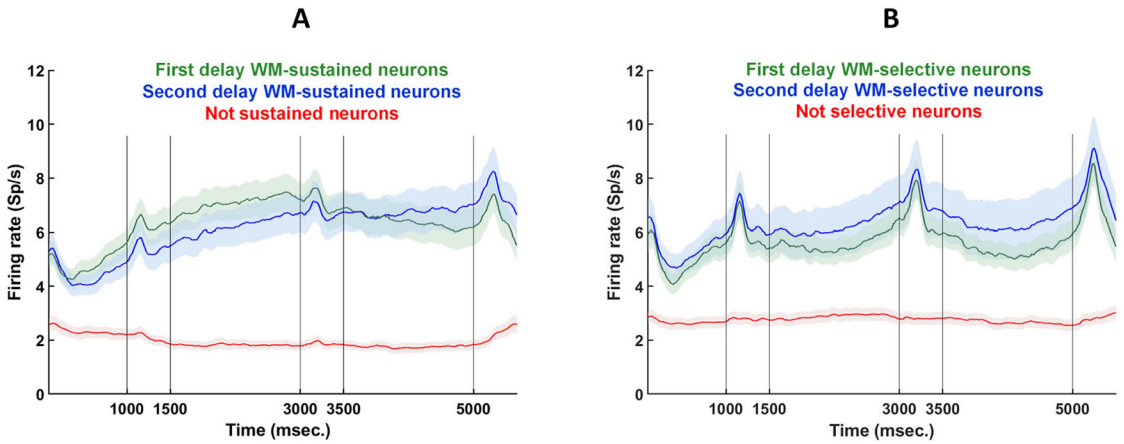

Fig. 2 | Firing rates of working memory-active neurons and non-active neurons in the spatial task. The mean firing rate was averaged across spatial stimuli for neurons classified as **A**) WM-sustained neurons and **B**) WM-selective neurons, based on firing rates in the first delay and second delay periods. $n = 233$, $n = 191$, $n = 449$ neurons for the first delay WM-sustained, the second delay WM-sustained, and the not sustained neurons, respectively. $n = 120$, $n = 124$, $n = 507$ neurons for the first delay WM-selective, the second delay WM-selective, and the not selective neurons, respectively. Data are represented as mean ± SEM.

compared across different stimulus locations to identify WM-selective neurons from 850 recorded neurons (one-way ANOVA, $p < 0.05$). A total of 120 neurons (20/171 [11.7%] in the posterior-dorsal, 85/321 [26.5%] in the mid-dorsal, and 15/358 [4.2%] in the posterior-ventral) and 124 neurons (25/171 [14.6%] in the posterior-dorsal, 82/321 [25.5%] in the mid-dorsal, and 17/358 [4.7%] in the posterior-ventral) were WM-selective to a specific location based on the first and second delay period firing rates, respectively. Importantly, during the second delay period, WM-selective neurons were identified based on their selectivity to either the location of the first or the second stimulus. On the other hand, 507 neurons (99/171 [57.9%] in the posterior-dorsal, 128/321 [39.9%] in the mid-dorsal, and 280/358 [78.2%] in the posterior-ventral) were classified as non-selective. Non-selective neurons did not exhibit significant firing rate differences in response to specific stimulus locations during any task epochs.

Our results revealed that there were more WM-sustained neurons than spatial WM-selective neurons in the recorded region of PFC: 233 vs. 120 neurons and 191 vs. 124 based on neuronal activity in the first and second delay periods, respectively. Additionally, 68% of WM-sustained neurons were sustained during both the first and second delay periods, and 62% of WM-selective neurons were common across both delay periods.

Notably, 26% (61 neurons) and 25% (48 neurons) of the WM-sustained neurons were also WM-selective during the first and second delay spiking activities, respectively (Fig. 1D). This indicated that although there was some overlap between WM-sustained and WM-selective neurons, the two populations did not fully coincide. In other words, there were WM-selective neurons that were not WM-sustained and vice versa. This distinction between WM-sustained and WM-selective was critical. WM-sustained neurons were identified by elevated firing activity during the delay periods, regardless of stimulus location selectivity, while WM-selective neurons exhibited significant firing rate differences to specific locations during the working memory epochs. The lack of a strict subset relationship suggested that a neuron can be sustained to the delay periods without being selective to a stimulus location.

Figure 2 illustrates the mean firing activity of WM-sustained and WM-selective neurons compared non-sustained and non-selective neurons, respectively. As expected, WM-sustained and WM-selective neurons exhibited significantly higher spiking activity than their non-active counterparts, confirming the effectiveness of our active neuron selection method.

Higher Fano factor in active PFC neurons

In this section, we sought to characterize neuronal response variability in monkeys during task performance. For this analysis, we focused on the Fano factor (FF), defined as the variance divided by the mean of neuronal spike counts[25–27]. The Fano factor was computed for WM-sustained, WM-selective, and non-active neurons, allowing for direct comparison across these populations (Fig. 3 and Supplementary Fig. 1). WM-sustained and WM-selective neurons based on the first delay period exhibited an increased Fano factor compared with non-active neurons (two-sided Wilcoxon rank-sum test, $p < 0.05$). The results were in line with a prior study finding on the response variability of PFC neurons[28]. Notably, the results were consistent across the analyzed PFC subdivisions (Supplementary Fig. 2) and across individual subjects (Supplementary Fig. 3). Active neurons according to the second delay firing rate also showed the same results (two-sided Wilcoxon rank-sum test, $p < 0.05$).

To further explore potential differences in neuronal selectivity during the second delay period, we compared the Fano factor of WM-selective neurons for the first and second stimulus locations (Supplementary Fig. 4). While the Fano factor was slightly higher for neurons selective to the first location compared to the second location, this difference was not statistically significant (two-sided Wilcoxon rank-sum test, $p > 0.05$). These findings support pooling neurons selective for the first and second stimulus locations for subsequent analyses.

Regardless of some differences between WM-sustained neurons and WM-selective neurons, both groups exhibited the same general trends in neuronal response variability as reflected in the Fano factor (Fig. 4). Furthermore, the comparison of Fano factor values between WM-sustained and WM-selective neurons showed no significant differences (Supplementary Fig. 5).

To control for the influence of neurons that were both WM-sustained and WM-selective during the first and second delay periods on the observed enhanced Fano factor, we recalculated the Fano factor after removing neurons common to both the WM-sustained and WM-selective sets. The number of exclusive WM-sustained and WM-selective neurons based on the first delay activity was 172 and 59, respectively, and based on the second delay activity was 143 and 76. Even when considering only these exclusive neurons, the difference in Fano factor between active neurons and non-active neurons persisted (Fig. 5).

Lower firing variability of working memory neurons in error trials

In this part of the study, we investigated the role of WM-sustained neurons and WM-selective neurons during trials in which monkeys chose the incorrect target. Figure 6 demonstrates the mean firing rate of WM-sustained and WM-selective neurons based on the first and second delay activity in error trials (i.e., incorrect decisions following the second stimulus presentation) compared to correct trials. Since there was no significant difference in firing rates of active neurons between correct and error trials, it

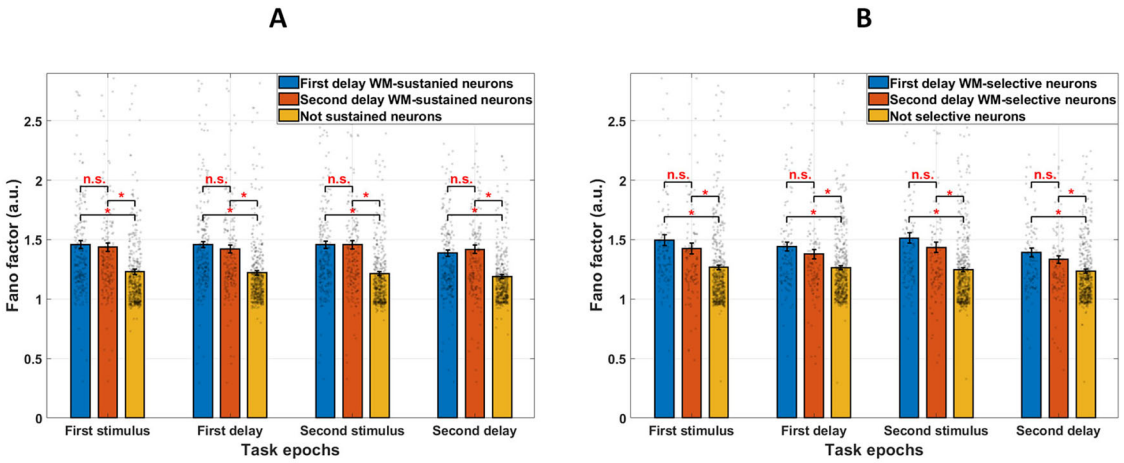

Fig. 3 | Response variability of working memory-active neurons and non-active neurons. Working memory-active neurons were identified based on the significant increase in firing rates during the first and second delay periods, and their Fano factors were measured. **A** WM-sustained neurons. **B** WM-selective neurons. $n = 233$, $n = 191$, $n = 449$ neurons for the first delay WM-sustained, the second delay WM-sustained, and the not sustained neurons, respectively. $n = 120$, $n = 124$, $n = 507$ neurons for the first delay WM-selective, the second delay WM-selective, and the not selective neurons, respectively. * Shows significant effects ($p < 0.05$), and n.s. stands for not significant based on the two-sided Wilcoxon rank-sum test. Gray dots represent individual data points for each unit. The vertical black lines represent ± SEM.

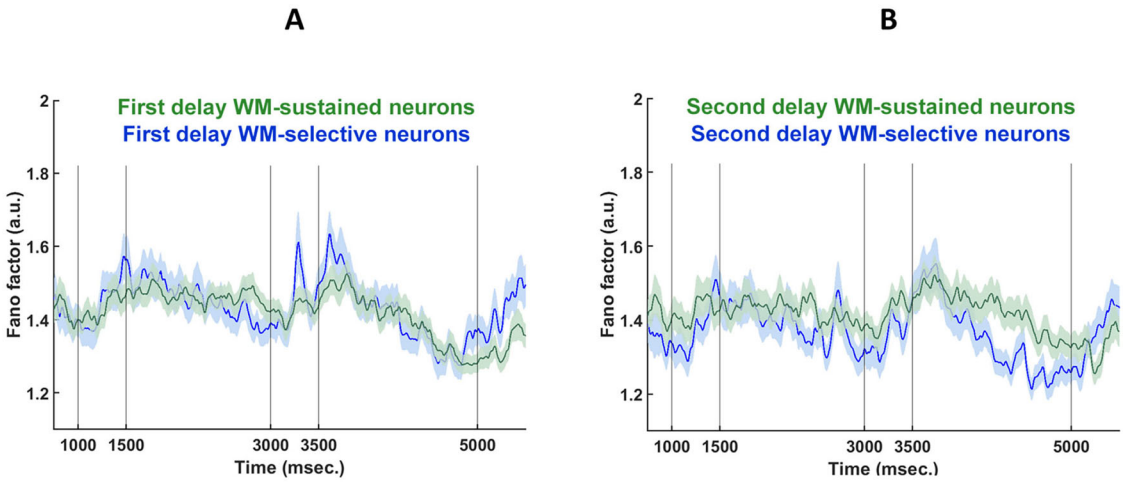

Fig. 4 | Comparison of response variability of working memory-active neurons. Working memory-active neurons were identified based on the significant increase in firing rates during the first and second delay periods, and their Fano factors were measured. **A** WM-sustained neurons. **B** WM-selective neurons. $n = 233$, $n = 191$ neurons for the first delay WM-sustained and the second delay WM-sustained, respectively. $n = 120$, $n = 124$ neurons for the first delay WM-selective and the second delay WM-selective neurons, respectively. Data are represented as mean ± SEM.

can be inferred that firing rate of active neurons was not the main factor contributing to the monkeys' incorrect decisions.

In the next step, the response variability of active neurons in error trials was calculated and compared with that in correct trials. Both WM-sustained and WM-selective neurons produced higher Fano factor in correct trials compared to error trials (Fig. 7). WM-sustained and WM-selective neurons based on the first delay period in correct trials showed an enhanced Fano factor compared with error trials (two-sided Wilcoxon rank-sum test, $p < 0.05$). Moreover, active neurons based on the second delay period activity also produced higher response variability in correct trials than incorrect ones (two-sided Wilcoxon rank-sum test, $p < 0.05$).

Spike phase coupling in working memory active PFC neurons

High-level cognitive functions such as working memory might be more sophisticated than just spike persistence, and neuronal populations as a network are more likely to be involved[29–31]. The locking of spiking activities to the phase of LFP oscillations (SPL) is a common method for determining the temporal coordination of individual neurons within a neuronal ensemble. The SPL approach determines the angular summation of LFP phases at spike times to assess the degree of locking of phases to spiking activities[32–34]. Many cortical regions, including the hippocampus[35], prefrontal cortex[36,37], motor cortex[38], and visual areas[39], have been shown to exhibit this type of coupling.

The fact that the value of SPL depends on spike numbers is an important constraint on the SPL estimate. Conditions with a higher number of spikes generate a lower SPL value[40,41]. To prevent any effects of the different numbers of spikes and trials of the two conditions, a fixed window of 20 spikes is considered, and the SPL magnitude for each window's spikes is measured before taking the mean across these windows[42]. Moreover, the phase value of each LFP was calculated based on a wavelet transform, and 100 ms after the stimulus offset in delay periods was excluded to avoid power contamination. The analyzed frequency range was 1–64 Hz, with a step of 1 Hz. The following conventional frequency bands were taken into account in the analysis: delta (2–4 Hz), theta (4–8 Hz), alpha (8–16 Hz), beta (16–32 Hz), gamma (32–40 Hz). While SPL in the frequency range of above

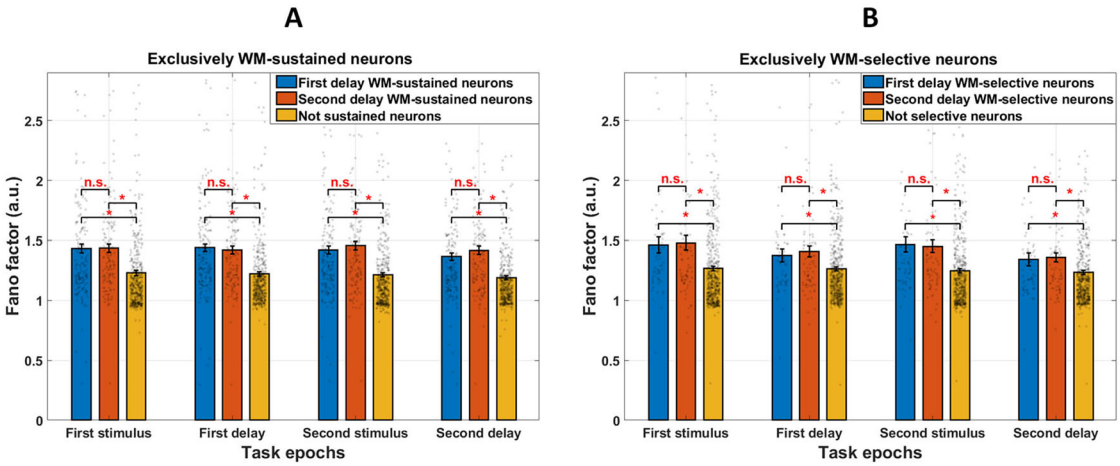

Fig. 5 | Response variability of exclusively working memory-sustained and selective neurons. Working memory-active neurons were identified based on the significant increase in firing rate during the first delay period and second delay periods, and their Fano factors were measured. **A** Exclusively WM-sustained neurons (not WM-selective neurons). **B** Exclusively WM-selective neurons (not WM-sustained neurons). $n = 172$, $n = 143$, $n = 449$ neurons for the first delay WM-sustained, the second delay WM-sustained, and the not sustained neurons, respectively. $n = 59$, $n = 76$, $n = 507$ neurons for the first delay WM-selective, the second delay WM-selective, and the not selective neurons, respectively. * Shows significant effects ($p < 0.05$), and n.s. stands for not significant based on the two-sided Wilcoxon rank-sum test. Gray dots represent individual data points for each unit. The vertical black lines represent ± SEM.

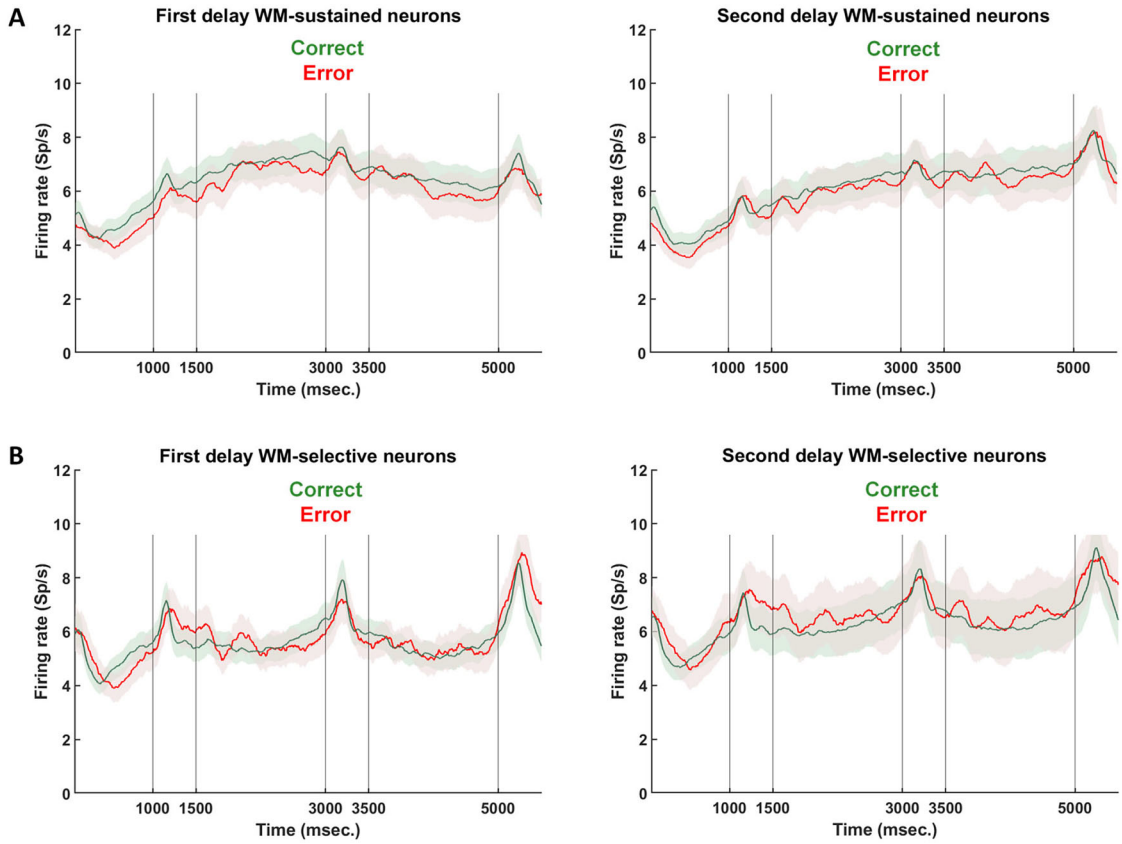

Fig. 6 | Firing rate of working memory-active neurons in correct and error trials. The mean firing rate was averaged across spatial stimuli for neurons classified as **A** WM-sustained neurons and **B** WM-selective neurons, based on the firing rates during the first delay and second delay periods. $n = 233$, $n = 197$ neurons for correct and error trials of the first delay WM-sustained neurons, respectively. $n = 191$, $n = 169$ neurons for correct and error trials of the second delay WM-sustained neurons, respectively. $n = 120$, $n = 104$ neurons for correct and error trials of the first delay WM-selective neurons, respectively. $n = 124$, $n = 104$ neurons for correct and error trials of the second delay WM-selective neurons, respectively. Data are represented as mean ± SEM.

~35 Hz did not show significant differences, it was thus excluded from detailed analysis to enhance clarity.

The analysis revealed that WM-sustained and WM-selective neurons induced a higher level of locking between the LFP phase and spike occurrence. Moreover, the increased SPL was more pronounced in active neurons selected based on the first delay firing rate compared to the firing rate of second delay period (Figs. 8 and 9). In alpha and beta bands, the first-delay-based WM-sustained and WM-selective neurons generated higher

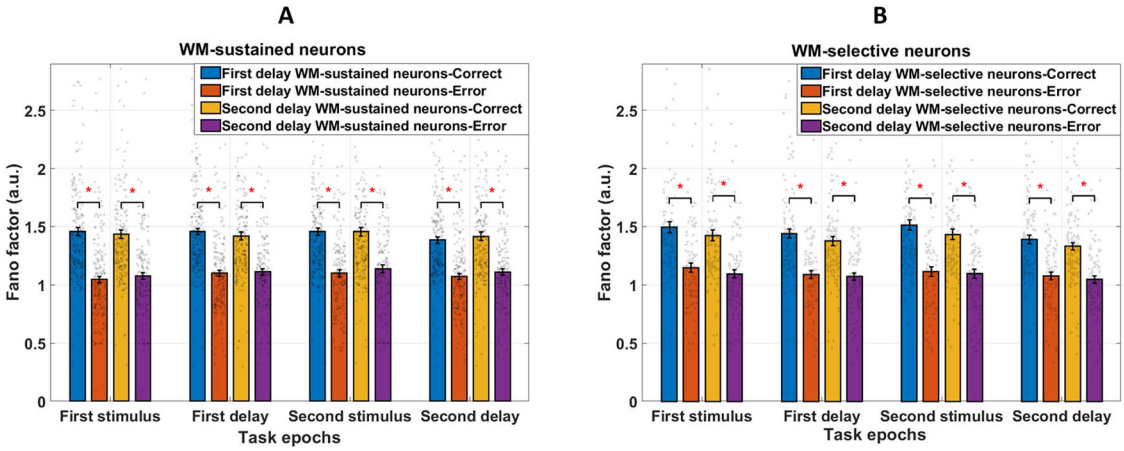

Fig. 7 | Response variability of working memory-active neurons in correct and error trials. The Fano factor of correct and error trials for first and second delay active neurons was calculated separately. **A** WM-sustained neurons. **B** WM-selective neurons. $n = 233$, $n = 197$ neurons for correct and error trials of the first delay WM-sustained neurons, respectively. $n = 191$, $n = 169$ neurons for correct and error trials of the second delay WM-sustained neurons, respectively. $n = 120$, $n = 104$ neurons for correct and error trials of the first delay WM-selective neurons, respectively. $n = 124$, $n = 104$ neurons for correct and error trials of the second delay WM-selective neurons, respectively. * Shows significant effects ($p < 0.05$) based on the two-sided Wilcoxon rank-sum test. Gray dots represent individual data points for each unit. The vertical black lines represent ± SEM.

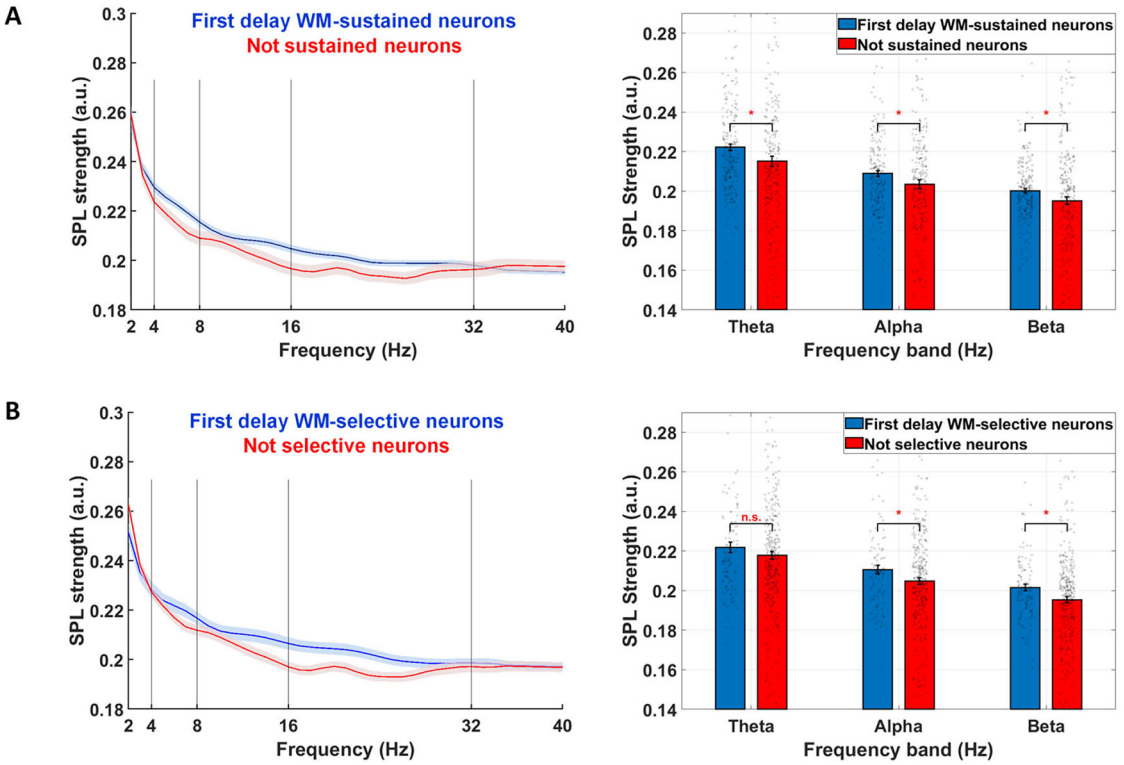

Fig. 8 | SPL of working memory-active neurons during the first delay epoch. SPL of first delay active neurons and non-active neurons was measured during the first delay period. **A** WM-sustained neurons. **B** WM-selective neurons. $n = 233$, $n = 120$ neurons for the first delay WM-sustained and the first delay WM-selective neurons, respectively. $n = 449$, $n = 507$ neurons for the not sustained and the not selective neurons, respectively. * Shows significant effects ($p < 0.05$), and n.s. stands for not significant based on the two-sided Wilcoxon rank-sum test. Gray dots represent individual data points for each unit. Data are represented as mean ± SEM.

SPL compared to non-active neurons (p-values of 1.9E-3 for the alpha band and 4.4E-3 for the beta band in WM-sustained neurons; and 4.8E-2 for the alpha band and 7.5E-3 for the beta band in WM-selective neurons; two-sided Wilcoxon rank-sum test). This effect was also observed for second delay-based WM-sustained and WM-selective neurons, although it was diminished and restricted to a narrower band (Fig. 9).

As a signature of interaction between neural population activity and single unit activity, SPL in correct and error trials was investigated to explore whether erroneous decisions were reflected in them. WM-sustained and WM-selective neurons exhibited stronger locking of spiking activity to the LFP phase in correct trials compared to error trials (Fig. 10 and Supplementary Fig. 6). This phenomenon was more pronounced in the theta, alpha and beta bands in WM-sustained and WM-selective neurons based on the first delay activity (p-values of 7.6E-5 for the theta band, 7.1E-3 for the alpha band, and 3.9E-02 for the beta band in WM-sustained neurons; and 2.1E-3 for theta band, 2.2E-3 for alpha band, and 6.6E-03 for beta band in WM-

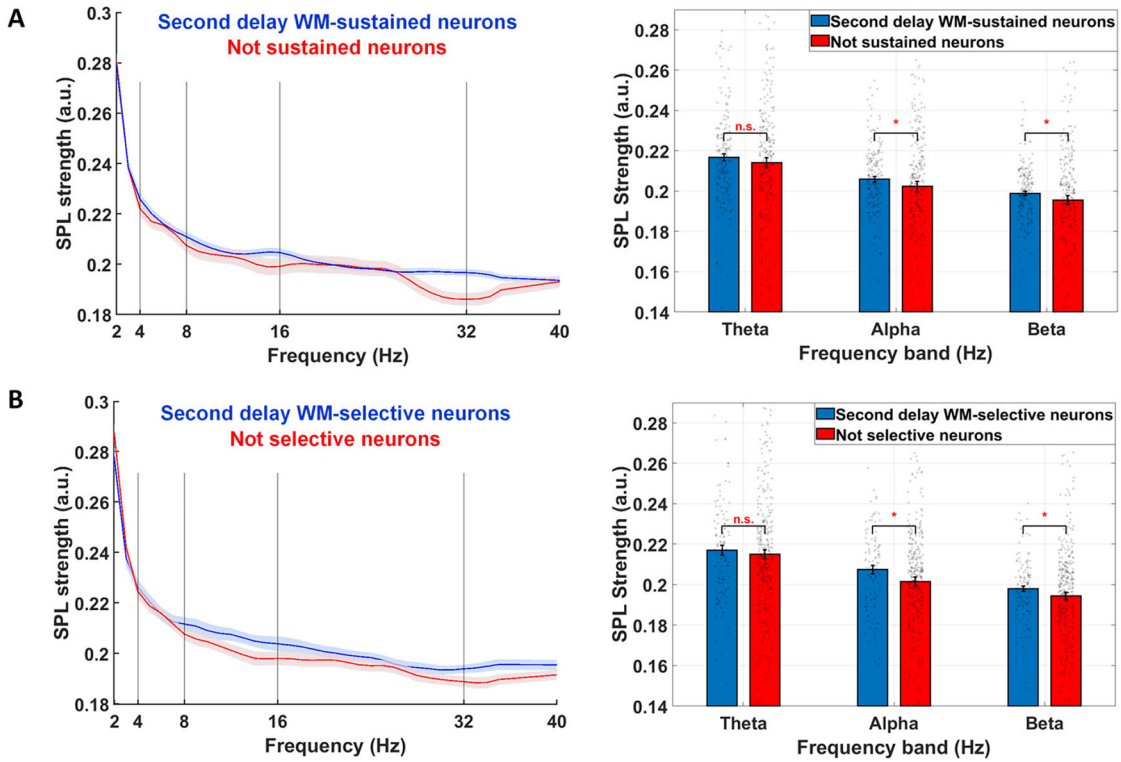

Fig. 9 | SPL of working memory-active neurons during the second delay epoch. SPL of second delay active neurons and non-active neurons was measured during the second delay period. **A** WM-sustained neurons. **B** WM-selective neurons. $n = 191$, $n = 124$ neurons for the second delay WM-sustained and the second delay WM-selective neurons, respectively. $n = 449$, $n = 507$ neurons for the not sustained and the not selective neurons, respectively. * Shows significant effects ($p < 0.05$), and n.s. stands for not significant based on the two-sided Wilcoxon rank-sum test. Gray dots represent individual data points for each unit. Data are represented as mean ± SEM.

selective neurons; two-sided Wilcoxon rank-sum test). Moreover, WM-sustained and WM-selective neurons identified based on the second delay activity also displayed stronger SPL during correct trials compared to error trials, but this effect was restricted to the beta band (p-values of 2.2E-3 in WM-sustained neurons and 2.3E-2 in WM-selective neurons; two-sided Wilcoxon rank-sum test). SPL analysis revealed that WM-sustained and WM-selective neurons showed similar patterns of synchrony with the LFP phase (Supplementary Fig. 6). However, the difference in SPL between correct trials and error trials was evident in active neurons identified based on the first delay activity. Furthermore, the coordination of spiking activity with the LFP phase of active neurons, particularly in the 14–22 Hz frequency range, distinguished correct from error trials.

Discussion

Enhancement of firing variability in working memory active neurons

Delayed response tasks include working memory gaps in time between sensory stimuli and making the decision based on the task rules. Increased neuronal activity is observed over delay periods in higher cortical regions, particularly PFC, suggesting that neurons are filling the delay periods by continuing to fire in response to task information[43]. The Fano factor, which quantifies neuronal variability, plays a significant role in understanding neuronal computation and cognitive processes. Research indicates that this variability is associated with attentional states and motor preparation, suggesting that the Fano factor serves as a marker for task engagement within neural circuits[44–46]. For instance, lower Fano factor values at stimulus onset often reflect stable encoding of sensory inputs, while higher variability may signal neural flexibility required for transitions between cognitive states[25,47]. In the context of working memory, the Fano factor is particularly significant because it reflects neural response modulations during the encoding and maintenance of task-relevant information[27,28,48]. These observations underscore the dependence of Fano factor dynamics on task context and the importance of variability in maintaining a balance between stability and flexibility in neural representation, which may ultimately enhance task performance[49].

It has been widely reported that neurons in sensory and association cortices, including the PFC, exhibit reduced variability (lower Fano factor) when actively processing stimuli. This reduction in variability has been proposed as a general property of the cortex[25,47]. This modulation is particularly evident in task-engaged neurons during attention, working memory, and decision-making tasks, where neurons actively encoding or maintaining information typically demonstrate reduced Fano factor during specific task epochs. This decrease in variability is thought to reflect stable task-related representations and the efficient processing of task demands[25,48].

In our study, we observed that working memory active neurons demonstrated a general reduction in Fano factor toward the end of the delay periods, in anticipation of the next task event (Fig. 4), consistent with prior findings[45]. However, we also identified a key distinction: working memory active neurons exhibited significantly higher response variability compared to non-active neurons. This suggests that while task-engagement stabilizes neural responses, active neurons maintain a level of variability to address task demands, reflecting their dynamic involvement in encoding and maintaining task-relevant information. In contrast, non-active neurons showed lower variability, indicating the difference in the level of engagement between the two neuronal populations.

Based on our results, active-neurons exhibited greater firing variability due to their responsiveness or selectiveness to task-related information. WM-selective neurons demonstrated higher activity for specific stimulus locations during delay periods. The higher Fano factors in selective neurons reflected the variability required to encode and maintain precise spatial information about stimuli. This spatial selectivity was crucial for the delayed match-to-sample task, as it involves the precise and variable encoding of specific locations.

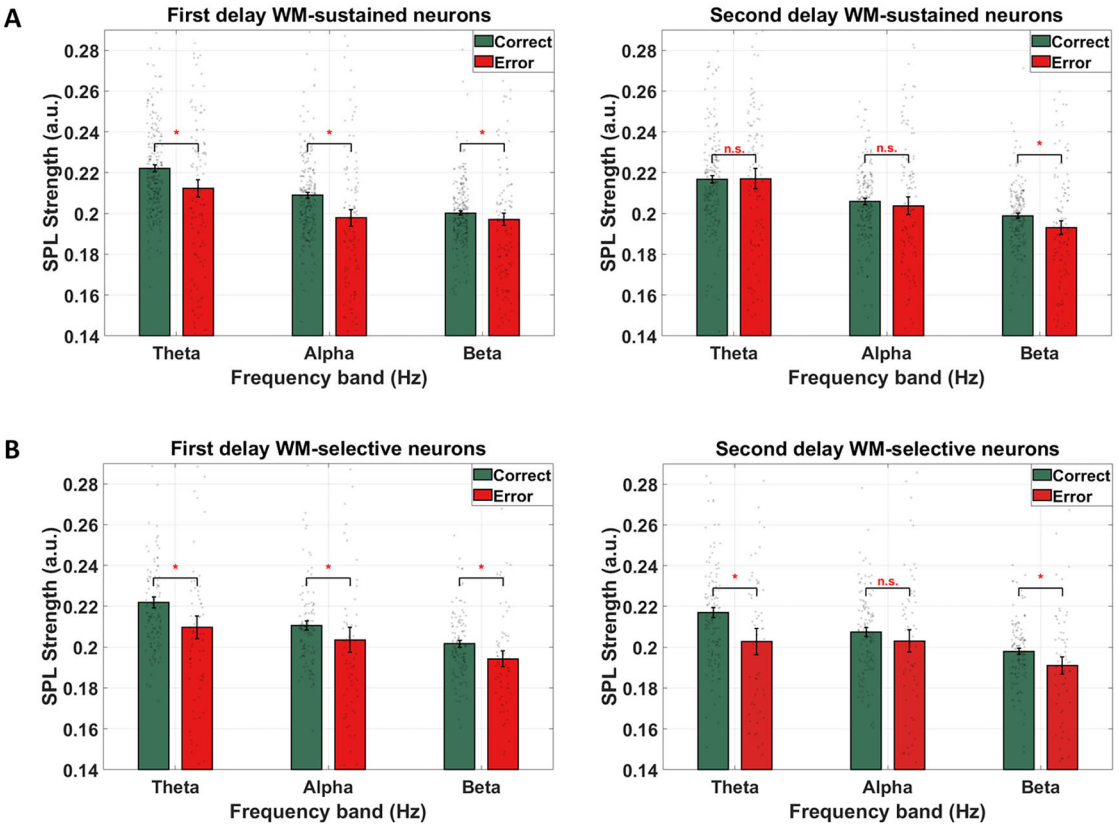

Fig. 10 | SPL of working memory-active neurons in correct and error trials. SPL of correct and error trials of first and second delay active neurons was calculated during the first delay period (left column) and the second delay period (right column). **A** WM-sustained neurons. **B** WM-selective neurons. $n = 233$, $n = 197$ neurons for correct and error trials of the first delay WM-sustained neurons, respectively. $n = 191$, $n = 169$ neurons for correct and error trials of the second delay WM-sustained neurons, respectively. $n = 120$, $n = 104$ neurons for correct and error trials of the first delay WM-selective neurons, respectively. $n = 124$, $n = 104$ neurons for correct and error trials of the second delay WM-selective neurons, respectively. * Shows significant effects ($p < 0.05$) and n.s. stands for not significant based on the two-sided Wilcoxon rank-sum test. Gray dots represent individual data points for each unit. The vertical black lines represent ± SEM.

In contrast, WM-sustained neurons exhibited increased firing activity during delay periods compared to fixation, possibly reflecting a role in maintaining general task-relevant information, which may not necessarily be tied to a specific location. Despite not exhibiting location-specific selectivity, their elevated neuronal variability suggests that they may contribute to the adaptive maintenance of information critical for task performance, supporting flexibility in response to the task demands. Future studies could investigate whether WM-sustained neurons are engaged across all working memory processes or play a more specific role, such as the representation of specific rules of individual tasks. This could be examined using targeted manipulations or task variations designed to dissociate these functions.

Non-active neurons were not engaged in the task actively and displayed baseline or background activity. In other words, they had generally more stable and less variable firing patterns. This stability was reflected in lower Fano factors, as they were not responding to the same degree of dynamic input and cognitive processing.

The lower Fano factors observed in WM-sustained and WM-selective neurons during error trials suggest that these neurons exhibit reduced firing variability when the task is not performed correctly. This reduction in variability may indicate a failure to engage cognitive control mechanisms, potentially limiting the flexibility needed for effective working memory maintenance during errors. While Hussar and Pasternak reported overall lower Fano factors during error trials compared to correct trials, they did not examine these changes separately for WM-sustained and WM-selective neurons[45]. Our findings provide new insights into the distinct roles of WM-sustained and WM-selective neurons, underscoring the critical role of neuronal variability in supporting the cognitive processes required for successful task performance.

It is worth noting that while high Fano factor values have been associated with greater variability and task engagement, prior research has also shown Fano factor quenching upon stimulus onset particularly in sensory neurons[25]. We observed this quenching phenomenon at the onset of the stimuli, where the Fano factor initially dropped. Following this, the Fano factor increased as the task progressed toward the delay periods. However, during delay periods, a decreasing trend in Fano factor was observed. Beyond this variation in the Fano factor across task epochs, active neurons exhibited dynamic task-related variability, as reflected in the elevated Fano factors observed in both WM-sustained and WM-selective neurons compared to non-active neurons. Therefore, although Fano factor quenching is a well-known phenomenon associated with sensory processing, the higher Fano factors observed in our study reflect the neural flexibility required for maintaining and manipulating working memory content, particularly during the delay periods.

Contributions of PFC's working memory neurons

The completion of goal-directed behavior tasks requires access to the wide range of information needed to identify potential goals and the rules that can achieve them. Despite the activation of many different brain areas, PFC is particularly crucial for executive functions[50]. Neurons in this region process information related to task-relevant stimuli and rules, maintain representations during working memory periods, and contribute to decision-making processes. It was suggested that to address a variety of cognitive functions, the selectivity of PFC neurons changes at the single-neuron level, according to the performed task[51].

The distribution of information in PFC neurons is affected by task information, and PFC has a crucial role in forming the representations of

task rules[2,52]. A prior study reported the sensitivity of PFC neural activity to rule information by varying task demands[19]. It was suggested that PFC is active during a wide range of cognitively demanding tasks as a part of the multiple-demand system, in contrast with brain regions that respond selectively to particular types of information[53]. In fact, task demands often influence PFC neural activity more than sensory inputs[16,54]. Moreover, training of complex cognitive tasks has a significant impact on the neuronal activity of PFC, and the number of task-activated neurons in the PFC increased after monkey task-learning[43,55].

Working memory is a complex process that involves the coordination of various cognitive functions over time, with neural networks supporting stimuli and task information, particularly during memory delays[56]. This complexity implies that different neuron types with distinct characteristics contribute to various aspects of the process. In this study, both WM-sustained and WM-selective neurons were modulated by working memory task demands. Although WM-sustained neurons were not selective to the spatial location of stimuli, their spiking variability was influenced by these demands. Working memory activity in the PFC likely involves processes that extend beyond specific stimulus characteristics including the maintenance of abstract representations, rule-based processing, and cognitive control.

Our findings suggest that both types of working memory active neurons contribute to the overall working memory process. While their roles may not be entirely distinct due to the similarity in Fano factors, the functional distinction lies in the specificity of their involvement: WM-selective neurons are likely more involved in encoding spatial information, whereas WM-sustained neurons may support more general task-related processes. Importantly, as non-selective neurons could still be sustained, they may play a role in supporting task-relevant information, as suggested by previous work[57]. These neurons may contribute indirectly to the information coding process, aligning with the idea that neural population coding benefits from including neurons that are not strictly tuned to stimulus features. This finding highlights the importance of considering a range of neuron types in population analyses, as their inclusion may reveal broader contributions to the robustness and efficiency of information processing.

Elevated alpha/beta spike-phase coherency of working memory neurons

Working memory serves as a crucial workspace for storing and processing information, making it essential for cognitive functions. Therefore, various mechanisms have been developed to enhance working memory. Previous studies have highlighted the fundamental role of cortical rhythms in regulating the task-dependent dynamics of working memory, suggesting these rhythms as key components of top-down control over thoughts[56].

Recent investigations in primates have shown that bottom-up signals emerge in the gamma band, while top-down influences predominantly occur in the low frequencies, particularly alpha and beta bands[58,59]. Furthermore, recent findings suggest that the alpha/beta top-down signals (8–30 Hz) inhibit the gamma band bottom-up signals (34–60 Hz)[31]. It is revealed that spiking activities, which periodically update the synaptic weight supporting memory maintenance, are mediated by the interaction of alpha/beta and gamma signals.

Spiking activities, crucial for preserving working memory content, have been linked to gamma-band activity[60]. Previous studies suggest that gamma-band activity is modulated by low-frequency top-down signals particularly in the alpha and beta bands[31,58]. This indicates that spiking may also be influenced by these low-frequency rhythms. Through this mechanism, the single-neuron activity interacts with the summed activity of neuronal populations, as reflected in LFPs. Adaptive changes in individual neuronal responses may, therefore, reflect broader network dynamics, optimizing population coding to meet diverse cognitive demands[61,62].

Alpha/beta band rhythms play a key role in PFC during cognitive functions such as executive control[63], working memory[64,65], and avoiding distraction[66]. Generally, low-frequency activity (10–30 Hz) is associated with the preservation of the current cognitive state and is crucial for working memory[67,68]. Our results illustrated that alpha/beta LFP phase and spiking activity interacted in working memory active neurons. According to the analysis, WM-sustained and WM-selective neurons exhibited significantly greater SPL than non-active neurons in the alpha and beta bands.

Moreover, a reduction in SPL in alpha and beta bands was evident in working memory active neurons during error trials. Our results were consistent with earlier research that assessed the impact of alpha/beta coupling on the performance of monkeys during task execution[31,64,69]. Poor coupling of spiking activity and the alpha/beta top-down signal was observed in error trials, suggesting that disruption in this coupling may contribute to working memory deficit. Our findings imply that working memory deficits can be reflected in the alpha/beta SPL and that patients with working memory-related disorders may benefit from interventions aimed at improving alpha/beta coupling.

Methods

In this article, we analyzed the neural data of two male macaque monkeys, aged 5–9 years and weighing 5–12 kg. None of these animals had ever been employed in any form of research before the experiment. The monkeys were housed either individually or in pairs within communal environments that allowed for sensory interactions with other monkeys. All experimental procedures were approved by the Wake Forest University Institutional Animal Care and Use Committee under protocol number A14-196 and followed the guidelines provided by the National Research Council's Guide for the Care and Use of Laboratory Animals and the U.S. Public Health Service Policy on Humane Care and Use of Laboratory Animals. The procedure was carried out as previously described[64,70]. We have complied with all relevant ethical regulations for animal use.

The monkeys were required to sit with their heads fixed in primate chairs, viewing a monitor that was 68 cm away from their eyes with low ambient illumination, and concentrate on a 0.2° white square that appeared in the center of the screen. Each trial started with a fixation period of 1000 ms. The monkeys were instructed to maintain their gaze on the fixation point during the presentation of visual stimuli, which were presented either at a peripheral location or over the fovea. After stimuli and delay periods, the monkeys were required to make a saccade to the correct choice. The correct performance of monkeys was rewarded with a drop of juice. The trial terminated immediately with any fixation break, with no reward. During the experiment, the subjects' eyes were continuously tracked using a non-invasive, infrared eye position scanning device (model RK-716; ISCAN, Burlington, MA). The system provided a resolution of 0.3° at the vision center. The eye position of subjects was sampled and recorded at a rate of 240 Hz. The Psychophysics Toolbox[71] and the MATLAB environment (Mathworks, Natick, MA) were employed to run custom programs that displayed visual stimuli, tracked eye position, and synchronized stimuli with neurophysiological data.

Behavioral task

Two macaque monkeys were trained to execute a spatial working memory task. At the start of each trial, a cue (the first stimulus) was presented for 500 ms, followed by a 1000 ms fixation period during which only a fixation point was displayed. Subsequently, a delay interval began with the fixation point remaining on the screen for 1500 ms. Thereafter, the second stimulus was presented for 500 ms. This stimulus could appear either at the same location as the first stimulus or at the directly opposite location. To maintain an equal number of match and non-match trials within the stimulus set, each cue was paired with exactly one non-match stimulus. After the presentation of the second stimulus, a 1500 ms delay period followed, during which only the fixation point remained visible. Finally, the monkeys were required to make a saccadic movement toward one of two target stimuli: green for a matching stimulus and blue for a non-matching stimulus. The target stimuli for each trial were pseudo-randomly presented at one of two orthogonal positions relative to the first/second stimuli. Importantly, the positions of the green and blue targets were not fixed across trials, eliminating any consistent association between target color and spatial position.

This task design ensured that the monkeys relied on their memory of the precise location of the first stimulus to determine whether the second stimulus matched it.

Surgery and neurophysiology

A circular craniotomy with a diameter of approximately 18 mm was carried out over the PFC, followed by the implantation of a recording cylinder. Anesthesia was induced with an intramuscular injection of ketamine (5 mg/kg) and maintained throughout surgery using 1–3% inhalant isoflurane. Following surgery, stereotaxic coordinates and anatomical magnetic resonance imaging (MRI) were employed to confirm the accurate placement of the cylinder. Electrode penetrations across the cortical surface were systematically mapped. Six distinct regions within the LPFC were identified: area 10 in the frontopolar region; area 45 in the posterior ventral region; area 8A in the posterior dorsal region; area 8B and area 9/46 in the mid-dorsal region; area 9 and area 46 in the anterior-dorsal region; and area 47/12 in the anterior-ventral region. Notably, the frontopolar and anterior subdivisions were under-sampled for the purposes of this analysis.

Neurophysiological recordings

Neural recordings were made in the previously indicated PFC areas during the spatial working memory task. To record extracellular signals, multiple glass- or epoxylite-coated tungsten microelectrodes with a diameter of 100–250 μm and a 1–4 MΩ impedance at 1 kHz (Alpha-Omega Engineering, Nazareth, Israel) were used. A microdrive system (EPS drive, Alpha-Omega Engineering) was employed to position arrays of up to eight microelectrodes, spaced 0.2 to 1.5 mm apart, through the dura mater and into the PFC. Signals from each electrode were amplified and filtered: spiking activity was band-pass filtered between 500 Hz and 8 kHz, while LFPs were filtered between 0.5 and 200 Hz, using a modular data capture system (APM system, FHC, Bowdoin, ME).

Data analysis

Neural data analysis was implemented with the MATLAB platform (R2020b, MathWorks, Natick, MA). To calculate the trial-averaged peristimulus time histograms, the spiking events were convolved at 50 ms intervals.

The firing rate of each neuron was calculated for each task period, separately. By applying a paired *t*-test, the neurons that exhibited a significant increase in firing rate during the delay periods (first and second delay periods separately) compared to the 1000 ms fixation interval were labeled as working memory-sustained neurons ($p < 0.05$). Using a one-way ANOVA test on the firing rates of each neuron during delay periods, neurons were identified as working memory-selective based on the significantly different responses to the spatial location of the stimulus.

To ensure robustness and minimize false positives, we applied additional criteria to identify WM-selective neurons: they were required to have a firing rate of at least 2 Sp/s for their best stimulus location during the task period in which the ANOVA test indicated a significant effect of stimulus location. Moreover, WM-sustained neurons were required to exhibit higher firing rates in the analyzed epoch compared to the fixation period. Neurons showing a significant decrease in firing rate were therefore excluded from the sustained category. We additionally required that a WM-sustained or WM-selective neuron exhibit a firing rate of at least 2 Sp/s during the analyzed delay period.

To study the trial-to-trial spike count variability, Fano factor was calculated[25]. The Fano factor, which is the variance relative to the mean of spike counts, was calculated as follows:

$$\text{Fano factor} = \frac{\text{var}(spike\ count)}{mean(spike\ count)}$$

We computed the Fano factor in each neuron using a 100 ms sliding window with a 10 ms stepping size. The calculated Fano factor in each window was assigned to the time point in the middle of the window. Then, Fano factors were averaged across neurons. The Fano factor was computed for each neuron across all correct trials, without separating trials by stimulus location. This approach was chosen to assess the overall trial-to-trial variability of neurons during task performance rather than condition-specific variability (Supplementary Figs. 7 and 8).

LFP recordings were preprocessed using custom code implemented in the MATLAB computational environment (2020b, Mathworks, Natick, MA). A band-pass filter (0.5–100 Hz) was applied for phase and amplitude extraction from the recording channels. We removed line power (60 Hz) and other artifacts from each electrode and trial of the LFP signal, if present.

To investigate SPL, the instantaneous phase value of each LFP signal was quantified using a complex Morlet wavelet transform. To avoid edge effects during stimulus presentation in working memory periods, 100 ms of the LFP signals after the stimulus offset in delay periods were excluded. The analysis frequencies ranged from 1 to 64 Hz in 1 Hz steps. After extracting the phase values using the wavelet analytic signal, a vector was created with the instantaneous phase at the spike time and an amplitude of one. The vector averaging method was applied to calculate the spike-phase locking magnitude.

$$SPL = 1/N\left|\sum_{n=1}^{N}\exp(i\varphi_n)\right|$$

where φ represents the LPF phase at which the spike occurred, and N is the number of spikes. To control for effects due to different numbers of spikes and trials and to capture a more stable effect, a fixed window of 20 spikes was considered[42]. The spikes from all trials of each neuron were pooled together. We measured the SPL magnitude for the spike times of each window and then took the mean across these windows.

Statistics and reproducibility

In this study, all statistical analyses were carried out using the MATLAB platform (R2020b, MathWorks, Natick, MA). To identify working memory-sustained neurons, a Wilcoxon signed-rank test was applied to compare firing rates during each delay period with the fixation period. To identify working memory-selective neurons, a one-way ANOVA was performed to assess the effect of stimulus location on firing rate during the delay periods. To compare neural variability across different groups, the Fano factor was computed for each neuron. Fano factors were then averaged within each task epoch (first stimulus, first delay, second stimulus, and second delay). The two-sided Wilcoxon rank-sum test was applied to compare the Fano factor between groups. For SPL analysis, SPL values were first calculated for each neuron and then filtered into theta, alpha, and beta frequency bands. The two-sided Wilcoxon rank-sum test was applied for comparisons between groups. A significance threshold of $p < 0.05$ was used for all statistical tests.

Reporting summary

Further information on research design is available in the Nature Portfolio Reporting Summary linked to this article.

Data availability

The source data used to generate all figures in this paper are provided in Supplementary Data 1. All other data supporting the findings of this study are available from the corresponding author upon reasonable request.

Received: 12 September 2024; Accepted: 12 May 2025;
Published online: 20 May 2025

References

1. Baddeley, A. Working memory: theories, models, and controversies. *Annu. Rev. Psychol.* **63**, 1–29 (2012).
2. Miller, E. K. & Cohen, J. D. An integrative theory of prefrontal cortex function. *Annu. Rev. Neurosci.* **24**, 167–202 (2001).

3. Just, M. A. & Carpenter, P. A. A capacity theory of comprehension: individual differences in working memory. *Psychol. Rev.* **99**, 122–149 (1992).
4. Baddeley, A. Working memory: looking back and looking forward. *Nat. Rev. Neurosci.* **4**, 829–839 (2003).
5. Engle, R. W., Tuholski, S. W., Laughlin, J. E. & Conway, A. R. A. Working memory, short-term memory, and general fluid intelligence: a latent-variable approach. *J. Exp. Psychol. Gen.* **128**, 309–331 (1999).
6. Vogel, E. K. & Machizawa, M. G. Neural activity predicts individual differences in visual working memory capacity. *Nature* **428**, 748–751 (2004).
7. Chatham, C. H. & Badre, D. Multiple gates on working memory. *Curr. Opin. Behav. Sci.* **1**, 23–31 (2015).
8. Funahashi, S., Bruce, C. J. & Goldman-Rakic, P. S. Mnemonic coding of visual space in the monkey's dorsolateral prefrontal cortex. *J. Neurophysiol.* **61**, 331–349 (1989).
9. Constantinidis, C. et al. Persistent spiking activity underlies working memory. *J. Neurosci.* **38**, 7020–7028 (2018).
10. D'Esposito, M. & Postle, B. R. The cognitive neuroscience of working memory. *Annu. Rev. Psychol.* **66**, 115–142 (2015).
11. Chaudhuri, R. & Fiete, I. Computational principles of memory. *Nat. Neurosci.* **19**, 394–403 (2016).
12. Zylberberg, J. & Strowbridge, B. W. Mechanisms of persistent activity in cortical circuits: possible neural substrates for working memory. *Annu. Rev. Neurosci.* **40**, 603–627 (2017).
13. Lara, A. H. & Wallis, J. D. The role of prefrontal cortex in working memory: a mini review. *Front. Syst. Neurosci.* **9**, 173 (2015).
14. Freedman, D. J., Riesenhuber, M., Poggio, T. & Miller, E. K. Categorical representation of visual stimuli in the primate prefrontal cortex. *Science* **291**, 312–316 (2001).
15. Shima, K., Isoda, M., Mushiake, H. & Tanji, J. Categorization of behavioural sequences in the prefrontal cortex. *Nature* **445**, 315–318 (2007).
16. Roy, J. E., Buschman, T. J. & Miller, E. K. PFC neurons reflect categorical decisions about ambiguous stimuli. *J. Cogn. Neurosci.* **26**, 1283–1291 (2014).
17. Nieder, A., Freedman, D. J. & Miller, E. K. Representation of the quantity of visual items in the primate prefrontal cortex. *Science* **297**, 1708–1711 (2002).
18. White, I. M. & Wise, S. P. Rule-dependent neuronal activity in the prefrontal cortex. *Exp. Brain Res.* **126**, 315–335 (1999).
19. Wallis, J. D., Anderson, K. C. & Miller, E. K. Single neurons in prefrontal cortex encode abstract rules. *Nature* **411**, 953–956 (2001).
20. Tang, H. et al. Prefrontal cortical plasticity during learning of cognitive tasks. *Nat. Commun.* **13**, 90 (2022).
21. Curtis, C. E. & Lee, D. Beyond working memory: the role of persistent activity in decision making. *Trends Cogn. Sci.* **14**, 216–222 (2010).
22. Rigotti, M. et al. The importance of mixed selectivity in complex cognitive tasks. *Nature* **497**, 585–590 (2013).
23. Meyer, T., Qi, X. L., Stanford, T. R. & Constantinidis, C. Stimulus selectivity in dorsal and ventral prefrontal cortex after training in working memory tasks. *J. Neurosci.* **31**, 6266–6276 (2011).
24. Riley, M. R., Qi, X. L. & Constantinidis, C. Functional specialization of areas along the anterior-posterior axis of the primate prefrontal cortex. *Cereb. Cortex* **27**, 3683–3697 (2017).
25. Churchland, M. M. et al. Stimulus onset quenches neural variability: a widespread cortical phenomenon. *Nat. Neurosci.* **13**, 369–378 (2010).
26. Mitchell, J. F., Sundberg, K. A. & Reynolds, J. H. Differential attention-dependent response modulation across cell classes in macaque visual area V4. *Neuron* **55**, 131–141 (2007).
27. Li, D., Constantinidis, C. & Murray, J. D. Trial-to-trial variability of spiking delay activity in prefrontal cortex constrains burst-coding models of working memory. *J. Neurosci.* **41**, 8928–8945 (2021).
28. Qi, X. L. & Constantinidis, C. Variability of prefrontal neuronal discharges before and after training in a working memory task. *PLoS One* **7**, e41053 (2012).
29. Miller, E. K., Lundqvist, M. & Bastos, A. M. Working memory 2.0. *Neuron* **100**, 463–475 (2018).
30. Lundqvist, M., Herman, P. & Miller, E. K. Working memory: delay activity, yes! persistent activity? Maybe not. *J. Neurosci.* **38**, 7013–7019 (2018).
31. Lundqvist, M., Herman, P., Warden, M. R., Brincat, S. L. & Miller, E. K. Gamma and beta bursts during working memory readout suggest roles in its volitional control. *Nat. Commun.* **9**, 394 (2018).
32. Lachaux, J. P., Rodriguez, E., Martinerie, J. & Varela, F. J. Measuring phase synchrony in brain signals. *Hum. Brain Mapp.* **8**, 194–208 (1999).
33. Vinck, M., Battaglia, F. P., Womelsdorf, T. & Pennartz, C. Improved measures of phase-coupling between spikes and the local field potential. *J. Comput. Neurosci.* **33**, 53–75 (2012).
34. Fries, P. A mechanism for cognitive dynamics: neuronal communication through neuronal coherence. *Trends Cogn. Sci.* **9**, 474–480 (2005).
35. Fernández-Ruiz, A. et al. Entorhinal-CA3 dual-input control of spike timing in the hippocampus by theta-gamma coupling. *Neuron* **93**, 1213–1226.e1215 (2017).
36. Voloh, B., Oemisch, M. & Womelsdorf, T. Phase of firing coding of learning variables across the fronto-striatal network during feature-based learning. *Nat. Commun.* **11**, 4669 (2020).
37. Siegel, M., Warden, M. R. & Miller, E. K. Phase-dependent neuronal coding of objects in short-term memory. *Proc. Natl. Acad. Sci. USA* **106**, 21341–21346 (2009).
38. Hall, T. M., Nazarpour, K. & Jackson, A. Real-time estimation and biofeedback of single-neuron firing rates using local field potentials. *Nat. Commun.* **5**, 5462 (2014).
39. Womelsdorf, T. et al. Orientation selectivity and noise correlation in awake monkey area V1 are modulated by the gamma cycle. *Proc. Natl Acad. Sci. USA* **109**, 4302–4307 (2012).
40. Vinck, M., van Wingerden, M., Womelsdorf, T., Fries, P. & Pennartz, C. M. The pairwise phase consistency: a bias-free measure of rhythmic neuronal synchronization. *Neuroimage* **51**, 112–122 (2010).
41. Zarei, M., Jahed, M. & Daliri, M. R. Introducing a comprehensive framework to measure spike-LFP coupling. *Front. Comput. Neurosci.* **12**, 78 (2018).
42. Bahmani, Z., Daliri, M. R., Merrikhi, Y., Clark, K. & Noudoost, B. Working memory enhances cortical representations via spatially specific coordination of spike times. *Neuron* **97**, 967–979.e966 (2018).
43. Miller, E. K. The "working" of working memory. *Dialog. Clin. Neurosci.* **15**, 411–418 (2013).
44. Cohen, M. R. & Maunsell, J. H. Attention improves performance primarily by reducing interneuronal correlations. *Nat. Neurosci.* **12**, 1594–1600 (2009).
45. Hussar, C. & Pasternak, T. Trial-to-trial variability of the prefrontal neurons reveals the nature of their engagement in a motion discrimination task. *Proc. Natl. Acad. Sci. USA* **107**, 21842–21847 (2010).
46. Riehle, A., Brochier, T., Nawrot, M. & Grün, S. Behavioral context determines network state and variability dynamics in monkey motor cortex. *Front. Neural Circuits* **12**, 52 (2018).
47. Ponce-Alvarez, A., Thiele, A., Albright, T. D., Stoner, G. R. & Deco, G. Stimulus-dependent variability and noise correlations in cortical MT neurons. *Proc. Natl. Acad. Sci. USA* **110**, 13162–13167 (2013).
48. Lundqvist, M. et al. Reduced variability of bursting activity during working memory. *Sci. Rep.* **12**, 15050 (2022).
49. Waschke, L., Kloosterman, N. A., Obleser, J. & Garrett, D. D. Behavior needs neural variability. *Neuron* **109**, 751–766 (2021).
50. Qi, X. L., Elworthy, A. C., Lambert, B. C. & Constantinidis, C. Representation of remembered stimuli and task information in the monkey dorsolateral prefrontal and posterior parietal cortex. *J. Neurophysiol.* **113**, 44–57 (2015).

51. Dang, W., Jaffe, R. J., Qi, X. L. & Constantinidis, C. Emergence of nonlinear mixed selectivity in prefrontal cortex after training. *J. Neurosci.* **41**, 7420–7434 (2021).
52. Fuster, J. M. Overview of prefrontal functions: the temporal organization of action. In *The Prefrontal Cortex (Fourth Edition)*. (ed. J. M. Fuster) 333–385 (Academic Press, 2008).
53. Duncan, J. The multiple-demand (MD) system of the primate brain: mental programs for intelligent behaviour. *Trends Cogn. Sci.* **14**, 172–179 (2010).
54. Cromer, J. A., Roy, J. E. & Miller, E. K. Representation of multiple, independent categories in the primate prefrontal cortex. *Neuron* **66**, 796–807 (2010).
55. Mansouri, F. A., Matsumoto, K. & Tanaka, K. Prefrontal cell activities related to monkeys' success and failure in adapting to rule changes in a Wisconsin Card Sorting Test analog. *J. Neurosci.* **26**, 2745–2756 (2006).
56. Buschman, T. J. & Miller, E. K. Working Memory Is Complex and Dynamic, Like Your Thoughts. *J. Cogn. Neurosci.* **35**, 17–23 (2022).
57. Zylberberg, J. Untuned but not irrelevant: The role of untuned neurons in sensory information coding. *bioRxiv* (2017).
58. Bastos, A. M. et al. Visual areas exert feedforward and feedback influences through distinct frequency channels. *Neuron* **85**, 390–401 (2015).
59. Michalareas, G. et al. Alpha-beta and gamma rhythms subserve feedback and feedforward influences among human visual cortical areas. *Neuron* **89**, 384–397 (2016).
60. Lundqvist, M. et al. Working memory control dynamics follow principles of spatial computing. *Nat. Commun.* **14**, 1429 (2023).
61. Chiang, F. K. & Wallis, J. D. Neuronal encoding in prefrontal cortex during hierarchical reinforcement learning. *J. Cogn. Neurosci.* **30**, 1197–1208 (2018).
62. Chiang, F. K., Wallis, J. D. & Rich, E. L. Cognitive strategies shift information from single neurons to populations in prefrontal cortex. *Neuron* **110**, 709–721.e704 (2022).
63. Wessel, J. R., Conner, C. R., Aron, A. R. & Tandon, N. Chronometric electrical stimulation of right inferior frontal cortex increases motor braking. *J. Neurosci.* **33**, 19611–19619 (2013).
64. Aliramezani, M., Farrokhi, A., Constantinidis, C. & Daliri, M. R. Delta-alpha/beta coupling as a signature of visual working memory in the prefrontal cortex. *iScience* **27**, 110453 (2024).
65. Schmidt, R. et al. Beta oscillations in working memory, executive control of movement and thought, and sensorimotor function. *J. Neurosci.* **39**, 8231–8238 (2019).
66. Zavala, B. A., Jang, A. I. & Zaghloul, K. A. Human subthalamic nucleus activity during non-motor decision making. Elife **6**, e31007(2017).
67. Engel, A. K. & Fries, P. Beta-band oscillations-signalling the status quo?. *Curr. Opin. Neurobiol.* **20**, 156–165 (2010).
68. Aliramezani, M., Singh, B., Constantinidis, C. & Daliri, M. R. Low-frequency local field potentials reveal integration of spatial and non-spatial information in prefrontal cortex. *Neuroimage* **310**, 121172 (2025).
69. Rezayat, E. et al. Frontotemporal coordination predicts working memory performance and its local neural signatures. *Nat. Commun.* **12**, 1103 (2021).
70. Riley, M. R., Qi, X. L., Zhou, X. & Constantinidis, C. Anterior-posterior gradient of plasticity in primate prefrontal cortex. *Nat. Commun.* **9**, 3790 (2018).
71. Meyer, T. & Constantinidis, C. A software solution for the control of visual behavioral experimentation. *J. Neurosci. Methods* **142**, 27–34 (2005).

Acknowledgements
Not applicable.

Author contributions
M.A., and M.R.D. conceptualized the current study; C.C. designed the behavioral task and provided the data; M.A. analyzed the data and prepared figures; M.A. wrote the manuscript; All authors interpreted the results, reviewed, edited, and approved the final version of the manuscript. M.R.D. supervised the study.

Competing interests
The authors declare no competing interests.

Additional information
Supplementary information The online version contains supplementary material available at https://doi.org/10.1038/s42003-025-08211-8.

Correspondence and requests for materials should be addressed to Mohammad Reza Daliri.

Peer review information *Communications Biology* thanks the anonymous reviewers for their contribution to the peer review of this work.

Reprints and permissions information is available at http://www.nature.com/reprints

Publisher's note Springer Nature remains neutral with regard to jurisdictional claims in published maps and institutional affiliations.

Open Access This article is licensed under a Creative Commons Attribution-NonCommercial-NoDerivatives 4.0 International License, which permits any non-commercial use, sharing, distribution and reproduction in any medium or format, as long as you give appropriate credit to the original author(s) and the source, provide a link to the Creative Commons licence, and indicate if you modified the licensed material. You do not have permission under this licence to share adapted material derived from this article or parts of it. The images or other third party material in this article are included in the article's Creative Commons licence, unless indicated otherwise in a credit line to the material. If material is not included in the article's Creative Commons licence and your intended use is not permitted by statutory regulation or exceeds the permitted use, you will need to obtain permission directly from the copyright holder. To view a copy of this licence, visit http://creativecommons.org/licenses/by-nc-nd/4.0/.

© The Author(s) 2025